UIDE

Powered by
Arizona State University

ING. MECATRÓNICA

Tesis previa a la obtención del título de Ingeniero en Mecatrónica.

AUTOR: Jean Carlo Collaguazo

TUTOR: Ing. Cristina Oscullo

Diseño e implementación de un prototipo para la extracción y almacenamiento automático de piezas impresas en 3D basado en detección de movimiento mediante visión artificial

Design and implementation of a prototype for the automatic removal and storage of 3D printed parts based on movement detection using artificial vision

QUITO – ECUADOR | 2023

CERTIFICATE OF AUTHORSHIP

I, Jean Carlo Collaguazo, hereby declare that this submission is my own work, it has not been previously submitted for any degree or professional qualification and that the detailed bibliography has been consulted.

I transfer my intellectual property rights to the Universidad Internacional del Ecuador, to be published and divulged on the internet, according to the provisions of the Ley de Propiedad Intelectual, its regulations and other legal dispositions.

Jean Carlo Collaguazo

ACKNOWLEDGMENTS

I would like to thank in a special way my parents who were my support throughout my university career, they supported me at all times and were there for me in every way, they are and always are the reason for my achievements in everything I do in my personal life and professional. I would also like to thank my friends with whom I traveled this long road to this point, who always knew how to be good friends inside and outside the university, and with whom I will always be grateful with all my heart, for every moment shared. Finally thank each one of my family members that I love them and they were always there for me. This has been a long journey that is just beginning, and I am fully prepared for new challenges.

CONTENTS

LIST OF FIGURES

LIST OF TABLES

DESIGN AND MATERIALS SELECTION

1. Analisys of alternatives

1.1. Selection of removal mechanism for 3D printed parts

There is a great selection in terms of 3D printing farms, and each one works differently, some carry out their processes with personnel in charge of supervising the operation of the printers and others that work automatically. For the selection of the mechanism for the removal of 3D printed parts, three 3D printing farm equipment was taken into consideration that have the same objective in their operation, to remove the finished parts from the hot beds of the 3D printers.

An analysis of alternatives was carried out to choose the most convenient equipment on which to base the operation.

Automated 3D printer farm

The 3D printer farm shown in Figure 1. works fully automatically, beginning by sending the g-code to the printers and removing and storing the finished parts. This 3D printing farm model works with 9 Prusa mk3 3D printers, this type of 3D printing farms are for industrial use and for mass production. However, it is designed to work only with one type of printer. These 3D printing farms are around $45,000, without counting the price of each printer.

Figure 1. Automated 3D printer farm [1]

3D printing farm from University of Agder

The 3D printing farm carried out at the University of Agder, works by moving the main structure in the X, Y and Z axis to remove the magneitc bed. It works by means an HMI which sends signal to the prototype for the removal of the 3D printed parts, this 3D printing farm uses rigid magnetic beds as mentioned before, which are removed and placed on a surface and subsequently using a brand new magnetic bed.

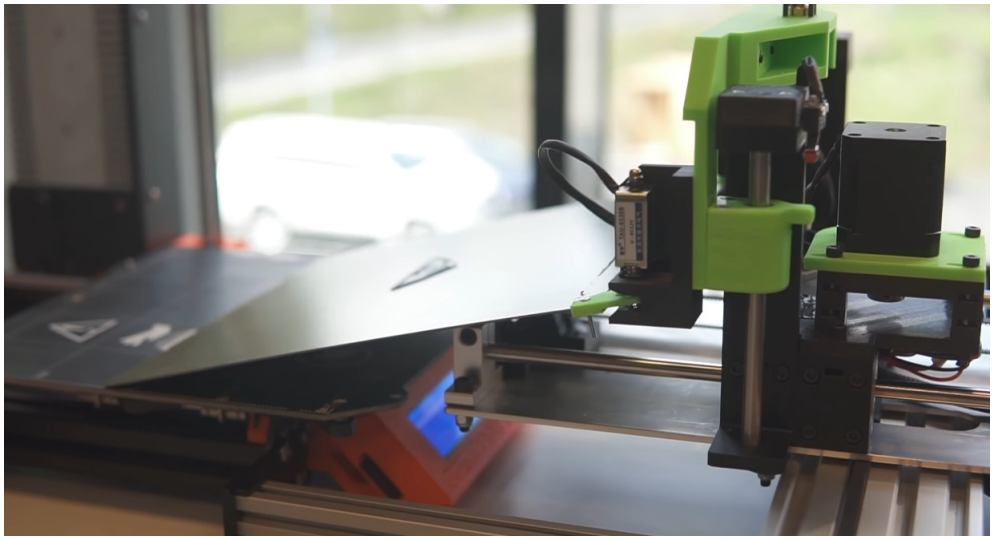

Figure 2. 3D printer from University of Agder [2]

3D Printing farm using the structure of the printers to detach the pieces

This type of 3D printing farms use the structure of the printers to remove the printed parts from the hot bed, modifying the G code to perform a removal routine at the end of the print. This type of farm does not present a cost in the short term, but it does in long term, since the pushing process forces the motors and reduces their useful life.

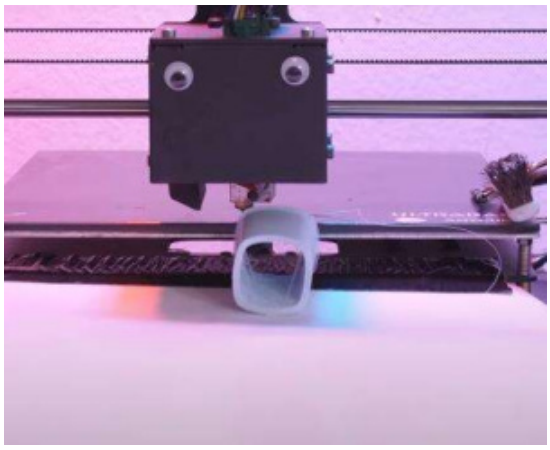

Figure 3. 3D Printing farm using 3D Printing [3]

After considering the 3D printing farm models, an analysis of alternatives is performed using the weighting criteria that Table 1 shows, and considering main characteristics of the 3D printer farms.

Table 1. Weighting table

Characteristic	**Weighing**
Very bad	1
Bad	2
Normal	3
Good	4
Very Good	5

Table 2. WEIGHTED CRITERIA MATRIX OF REMOVAL PART METHODS

Criteria					
Removal part method	**Cost**	**Speed**	**Efectivity**	**Maintenance**	**Score**
Automated 3D printer farm	1	5	5	5	16
3D printer from University of Agder	3	5	5	5	18
3D Printing farm using 3D Printing	5	4	1	1	11

After carrying out the analysis of alternatives and considering the main characteristics of the 3D printing farms, it can be seen that the alternative that has the best weighting is the 3D printing farm carried out at the University of Agder, for which the design will be carried out based on the mentioned model.

2. Heated bed selection

For the removal of the piece from the hot bed of the 3D printer, different hot beds available on the market were taken into account, considering as the main characteristic the force necessary to remove the piece from the surface and as a second point its manipulability. Taking into account the 3 most used hot beds today, a comparison was made of the force required to remove a standard piece from each heated bed [5] as can be seen in Table3.

Table 3. Force required to remove part from heated beds.

Heated bed	Force required to remove a 3D printed piece [N]
Rigid magnetic bed	3.13
Soft magnetic bed	13.94
Carborundum glass bed	23.04

Considering that to remove a piece from the rigid magnetic bed, no more than a quarter of the force required in the other beds is needed, it was used for the final prototype, obtaining satisfactory results in the detachment of the pieces.

3. Mechanical Design

The prototype design was made based on the model of the 3D printing farm made at the Adger University (Figure 2). Once the design was made, the respective mechanical calculations were made to determine the necessary torques to move the X, Y and Z axis (Figure. 4) and select the motors accordingly.

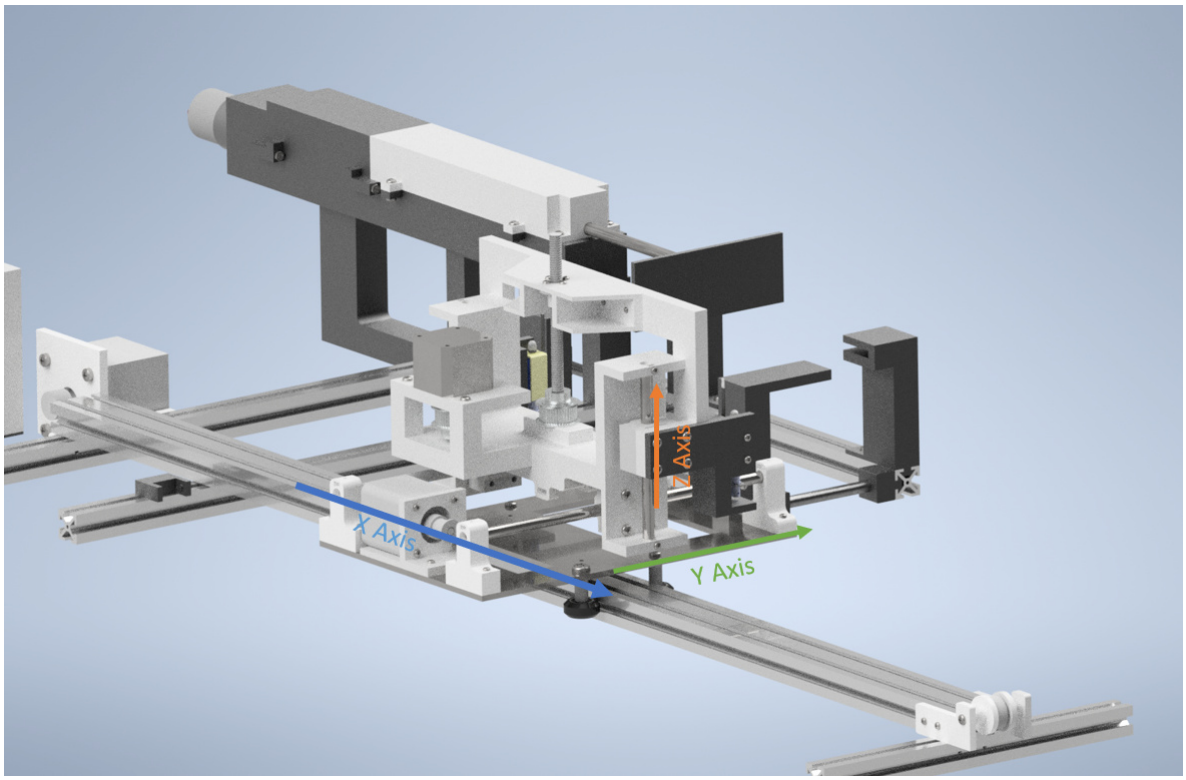

Figure 4. Prototype axes

The weight of each structures carried by each axis is calculated in Table 4 easily by using equation (1)

$$Weight = mass * gravity \tag{1}$$

to calculate the torque of each motor.

Table 4. Weights obtained from the axis structures

Structure axis	Mass (Kg)	Weight(N)
X	2.9	38.42
Y	1.5	24.52
Z	0.7	16.66

3.1. X axis motor sizing

Since the transmission system of the X axis is a pulley-belt, the free body diagram shown in Figure 5 is considered.

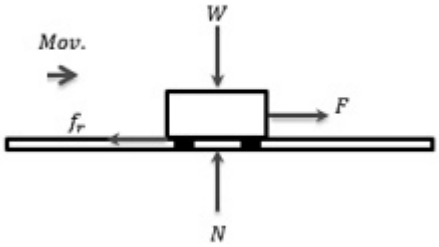

Figure 5. X axis free body diagram

To calculate the force necessary to move the structure in the X axis, the kinetic energy equation (Equation (2)) [6] is used.

$$T = \frac{1}{2}mv^2 \tag{2}$$

In addition:

$$W = F * d \tag{3}$$

$$F = F - f_r \tag{4}$$

$$f_r = \mu_k * N \tag{5}$$

Where:

T=Kinetic energy

W=Work

μ_k=Friction factor

N= Normal force

v= Speed of displacement

d= Distance between pulleys

g= Gravity

f= Frictional force

F=Force required to move the structure

Taking into account that the calculated weight of the X axis is 38.42 N. The force required for move the X axis structure is calculated with equation (6).

$$F_x = N_x * (\frac{v_x^2}{2 * d_x * g} + f_r) \quad (6)$$

Where:

N_x= Normal force on X axis (38.42 N)

v_x= speed of X axis structure (85 mm/s)

d_x= distance between pulleys (1.75 m)

g= gravity (9.81 m/s)

f_r= Frictional force (μ_k=0.52)

Substituting the values in equation (6) we obtain:

$$F_x = 38.42 * (\frac{0.085^2}{2*1.75*9.81} + 0.52)$$

$$F_x = 19.98N$$

Therefore, to calculate the motor torque required to move the X axis structure, we neglect the weight of the belt and the inertia generated by the pulleys, so we use equation (7).

$$\tau = F * r \quad (7)$$

Where:

F_x= Force calculated

r_x = Pulley radius

Then,

$$\tau_x = 19.98N * 0.02m = 0.39N.m$$

A 0.97 N.m torque motor is used to smoothly move the X-axis platform.

3.2. X axis motor selection

Once the necessary torque for the X axis was calculated, the Nema 23 motor was chosen to move the structure. The specific model used is the Nema23-KH56KM2U121, which was bought because of its low price and high torque. Considering the main characteristics of this Step motor [7] (Table 5).

Table 5. X Axis Nema 23 main characteristics

Model	KH56KM2U121
Step angle	1.8
Rated current [A]	2
Holding torque [N.m]	0.97

Comparing with the torque calculated for the x-axis, it can be seen that the chosen motor is stronger than the required torque, this providing greater security, and smoother movements without forcing the motor in any way. In addition to being one of the most used for this type of application due to its availability in the market and low cost.

3.3. Deformation analysis on main beam

Considering that the aluminum profile located on the X axis will support the weight of the entire structure that transports the magnetic bed and the printed parts, a simulation is performed in the Autodesk Inventor deformation analysis software as shown in Figure 6. to verify that the main axis will not suffer deformation due to the weight and does not need additional support for its correct operation.

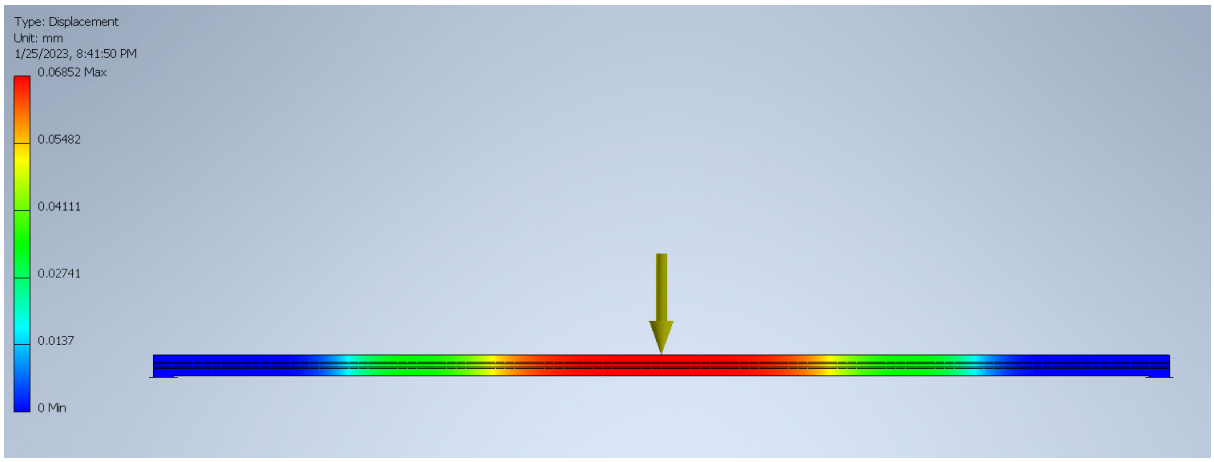

Figure 6. Analysis of deformation in the X axis

After carrying out the deformation simulation, it can be seen that it has a deformation value of 0.09mm, which is negligible due to its small value since it will not affect the main beam.

3.4. Y axis motor sizing

Considering that the transmission system of the Y axis structure is likewise of the belt-pulley type, the same procedure is carried out as with the X axis, then usign equation (6):

N_y= 38.42 N

d_y= 0.2 m

$$F_y = 38.42 * (\frac{0.05^2}{2*0.15*9.81} + 0.18)$$
$$F_y = 6.94N$$

And finally to get the torque of the Y axis motor, equation(7) is used, obtaining:

$$\tau_y = 6.94N * 0.012m = 0.083N.m$$

3.5. Y axis diameter shafts sizing

Considering that the weight on the Y axis is 14.7 and is distributed in two support axis of 20cm each. We can calculate the bending moment using the equation (8):

$$M_y = \frac{F_y * L_y}{4} \tag{8}$$

Where:

F_y= Applied force

L_y= Shaft length

Substituying:

$$M_y = \frac{7.35*0.2}{4} = 0.36N.m$$

and finally to obtain the diameter of the shaft, the equation (9) is used

$$d_y \geq (\frac{32 * N * M_y}{\pi * S_y})^{1/3} \tag{9}$$

Where:

S_y= Yield strength of steel

N=Security factor substituting:

$$d_y \geq (\frac{32*2*0.36}{\pi*205})^{1/3}$$

$$d_y \geq 3.57mm$$

3.6. Y axis motor selection

Once the necessary torque for the Y axis was calculated, the Nema 17 motor was chosen to move the structure. The specific model used is the Nema17-Kh42km2r075, which was bought because of its low price and availability. Considering the main characteristics of this Step motor(Table 6).

Table 6. Y axis Nema 17 main characteristics

Model	Kh42km2r075
Step angle	1.8
Rated current [A]	1.2
Holding torque [N.m]	0.39

Comparing with the calculated torque for the Y axis, it can be seen that the chosen motor is stronger than the required torque, this providing greater security, and smoother movements without forcing the motor.

3.7. Z axis motor sizig

Considering that the mechanism used for the Z axis is a power screw, and that this is in charge of lifting the structure of the z axis and also the printed part, the motor otorque is calculated for a critical case in which the printed part weighs 1kg. Therefore, the maximum weight that this axis would lift is 16.67N. Then, to calculate the torque of the motor that uses the Z axis, the equation (10) is used:

$$T_u = \frac{F * D_p}{2}[\frac{\cos(\emptyset) * \tan(\lambda) + f}{\cos(\emptyset) - f * \tan(\emptyset)}] \tag{10}$$

Where:

Force to move: $F_z = 16.66N$

pitch diameter:$D_p = 6.92mm$

Coefficient of friction:$f = 0.19$

Thread angle:$\phi = 30$

Lead angle:$\lambda = 1.9$

Substituying:

$$T_z = 0.067\ Nm$$

3.8. Z axis motor selection

Once the necessary torque for the Z axis was calculated, the Nema 17 motor was chosen to move the structure. The specific model used is the Nema17-HS3401, which was bought because of its low price and availability. Considering the main characteristics of the motor [8] (Table 7).

Table 7. Z axis Nema 17 main characteristics

Model	HS3401
Step angle	1.8
Rated current [A]	0.8
Holding torque [N.m]	0.28

Comparing with the calculated torque for the Z axis, it can be seen that the chosen motor is stronger than the required torque, this providing greater security, and smoother movements without forcing the motor.

3.9. Linear actuator

The necessary torque for the linear actuator motor is calculated, taking into account that in a critical case the actuator has to be able to push a 1kg piece.

For the construction of the power screw, the same threaded axis was used as in the z axis, so we used the same data taken from the datasheet, and using equation (6):

Where:

Force to move: $F_z = 9.81N$

pitch diameter:$D_p = 6.92mm$

Coefficient of friction:$f = 0.19$

Thread angle:$\phi = 30$

Lead angle:$\lambda = 1.9$

Substituying:

$$T_z = 0.039\ Nm$$

Due to availability, the JGB37-520 motor is used since it has a torque of 1 N.m and satisfies the calculation made.

4. Electrical Design

4.1. Power supply Sizing

For the power supply of the prototype electronic components, a sizing of the power source was carried out, so that the control circuit works optimally, and does not have problems of lack of voltage or current, below in Table 8 you can see the voltage and current consumption of each of the electronic components that the prototype has and finally determine the total current consumption and the different supply voltages that the control circuit needs.

Table 8. Power Consumption of each Electronic Component

Component	Quantity	Voltage[V]	Current [A]
Microcontroller: Arduino Mega	1	12	0.02
NEMA 17 HS3401	1	12	0.8
NEMA 17 Kh42km2r075	1	12	1.2
NEMA 23 KH56KM2U121	1	12	2
Raspberry PI3B+	1	12	0.9
DRV8825	3	12	6.6
IRF540	1	12	1.6
Solenoid Electromagnet	2	12	0.6
Webcam	2	5	3
TOTAL			**18.32**

Considering the calculation made of the current that the power supply will consume, a voltage source with 3 outputs 12, 5 and 3v of 30A is used for the prototype.

4.2. Circuit architecture

Once the current to be used for the circuit is obtained, it is important to define the connections between the components before designing the PCB, for which a block diagram is made in which the connections and the voltage of the circuit are defined. power supply of the components to be used.

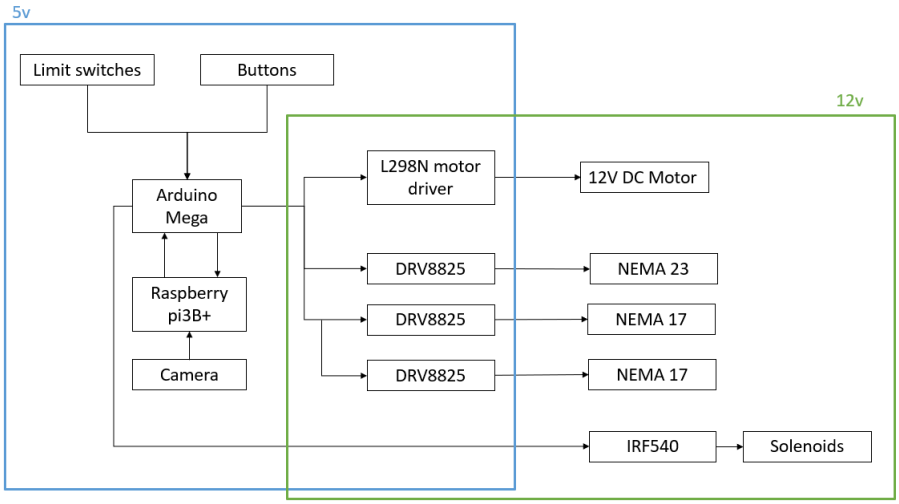

Figure 7. Main circuit operating architecture

4.3. Calculation for stepper motor drivers

To control stepper motors, the DRV8825 drivers are used, which work with a maximum current of 2.5A, however, these devices do not work all the time with their maximum current, for which they have an internal potentiometer to limit the flow of current. To find this maximum current with which the stepper motor will work, use the equation(11) [9].

$$I_{max} = \frac{V_{ref}}{5 * Rs} \tag{11}$$

Using the built-in potentiometer we are going to regulate the V_{ref} to limit the current. To get the V_{ref} we have to solve for equation 11, then we obtain 12:

$$V_{ref} = I_{max} * (5 * Rs) \tag{12}$$

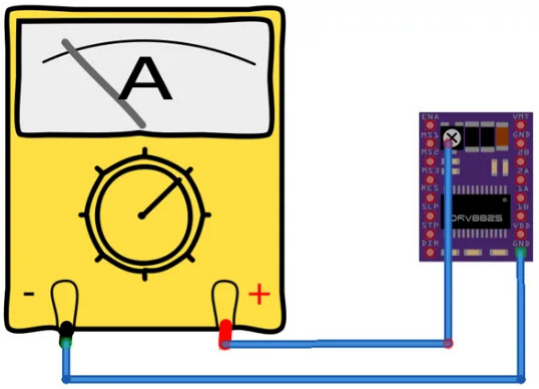

Figure 8. Measure V_{ref} on DRV8825 [4]

Calculation of V_{ref} for X axis stepper motor

Considering Stepper motor maximum current $I_{max} = 2A$

it have to work with 0.1 A less to avoid working with the limit of the motor, obtaining:

$$V_{ref} = 1.9 * 5 * 0.1 = 0.95V \tag{13}$$

Calculation of V_{ref} for Y axis stepper motor

Considering Stepper motor maximum current $I_{max} = 1.2A$

it have to work with 0.1 A less to avoid working with the limit of the motor, obtaining:

$$V_{ref} = 1.1 * 5 * 0.1 = 0.55V \tag{14}$$

Calculation of V_{ref} for Z axis stepper motor

Considering Stepper motor maximum current $I_{max} = 0.8A$

it have to work with 0.1 A less to avoid working with the limit of the motor, obtaining:

$$V_{ref} = 0.7 * 5 * 0.1 = 0.35V \tag{15}$$

After obtaining the reference voltages, we proceed to measure as shown in Figure 8

4.4. PCB Design

For the control circuit, the first design was designed and implemented in Proteus as Figure 9 and later, testing the connections to verify that the entire prototype works in a corresponding way, with the functional tests of the electronic components.

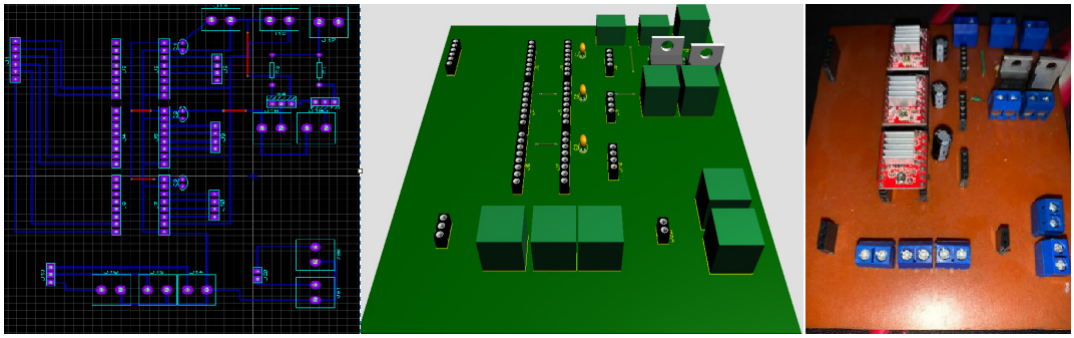

Figure 9. First implemented circuit

Once it was verified that the control circuit worked correctly, a shield was made to make the circuit more compact, occupy less space and considering that the final prototype is totally modular. Finally, after the design, it was manufactured and finished as shown in Figure 10.

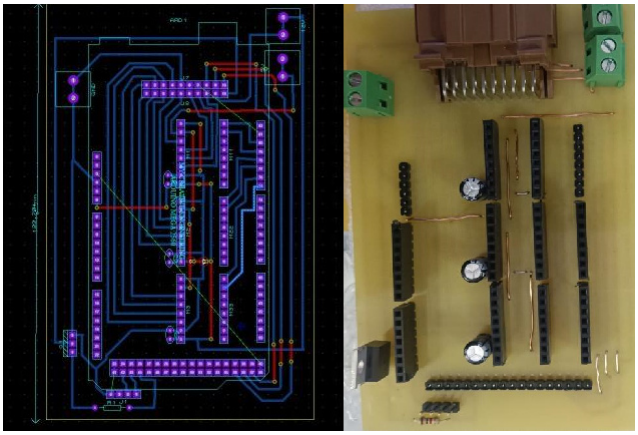

Figure 10. Final implemented circuit

5. Artificial Intelligence Component

For the artificial intelligence component, an artificial vision system is implemented for the detection of movements using image processing. The artificial vision system works with 2 cameras, that is, one for each printer, and they are placed on top of the printers in the aluminum structures as shown in Figure 11.

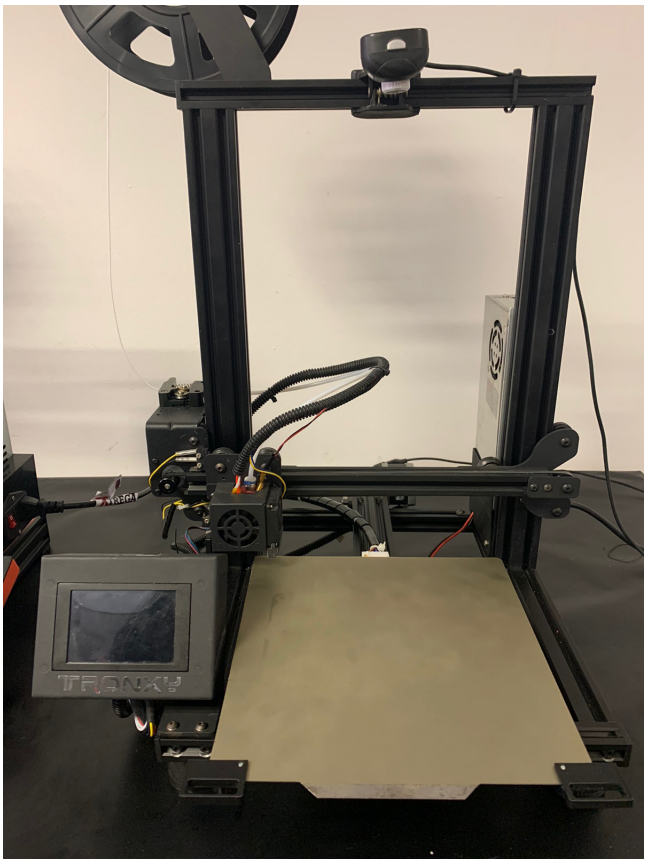

Figure 11. Location of cameras for movement detection

It's placed in the aluminum structure since it can capture all the movements made by the printers.

To develop the movement recognition program, python and the Open cv library were used for image processing, later the capture of both cameras was obtained, then the image was changed to grayscale and finally subtracted from the capture of the background or the image obtained from the camera to detect when it's moving.

To finish, squares are drawn on the contours of the moving object as shown in Fig.12 so that it can be better visualized.

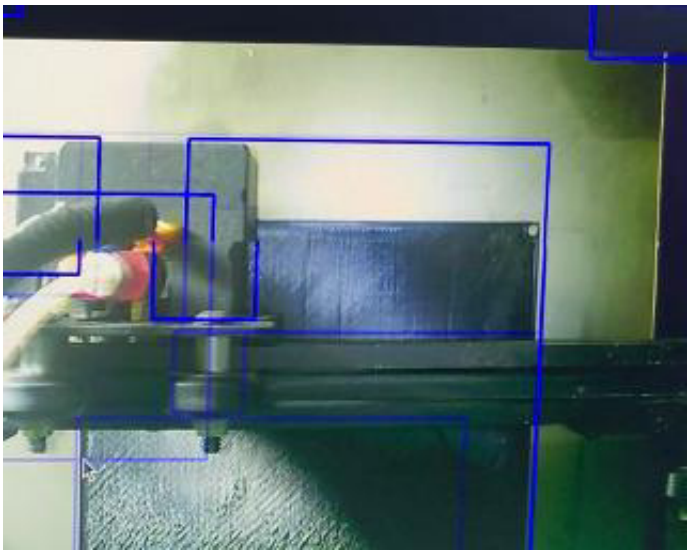

Figure 12. Movement detection program

During the tests of the operation of the motion detector, the presence of false positives was observed in the detection of one of the two cameras. These false positives occurred in very small areas of the image. After investigating the problem, it was inferred that the cause of these false positives was noise present in the image. This noise occurs when the ambient light available is insufficient [10], making it difficult for the camera sensors to correctly capture the light signal. As a result, random patterns of colored pixels appear in the image, affecting the clarity and accuracy of detection. To solve this problem, two actions were carried out: the first was to improve the illumination to increase the amount of light available, and the second was to resize the image before processing it in the detector, in order to remove noise pixels. These actions made it possible to solve the problem of false positives in the movement detector. Once the movement detection program was carried out, a counter was added which goes up to 50 to detect when a printer has completely stopped, this is because in the middle of the prints there are millimeter movements made by the printers that the camera cannot capture, so this timer helps to make sure that 3D printer stops working, also the heated bed lowers its temperature and its help to revome easily the 3d printed parts. To better understand how the motion detection algorithm works, Figure 13 is presented.

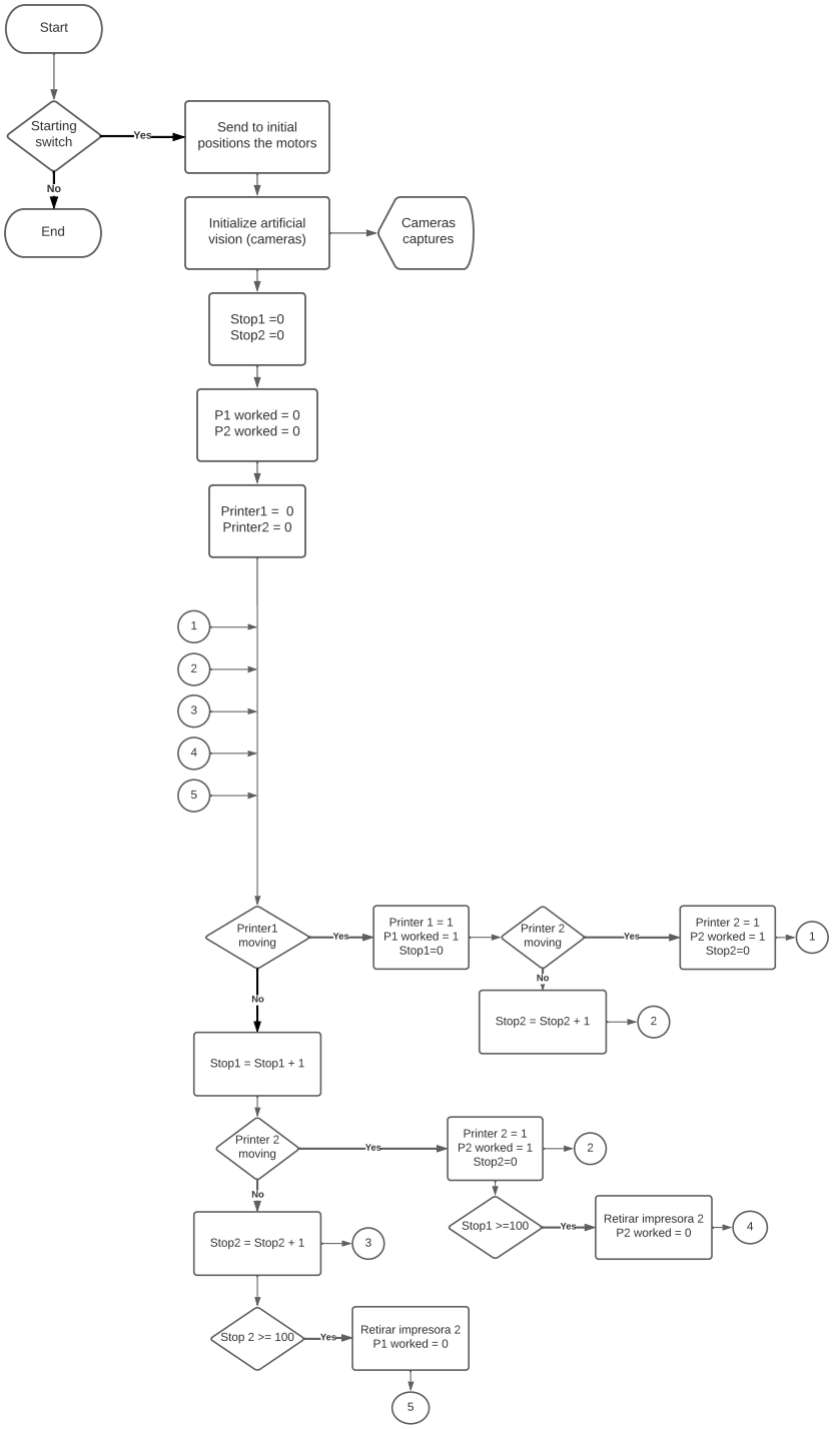

Figure 13. Flowchart of the logic of operation of the artificial vision algorithm

6. Expenses

Table 9 includes a summary of the expenses used during the construction of the prototype.

Table 9. Expenses done throughout the project

Element	Quantity	Price per Unit[$]	Total Price [$]
threaded rod and coupling	1	16	16
Bearings 22x8cm	3	3.5	10.5
Bearings 6x3cm	1	7	7
Bolts and nuts	1	10	10
Aluminum profile 1.7m	1	27.60	27.60
Aluminum profile 1m	2	10	20
Power supply 12V 10A	1	15	15
Microcontroller: Arduino Mega	1	20	20
640 RPM - 12v DC Motor	1	15	15
Nema 23	1	20	20
Nema 17	2	7	14
Aluminum profile coupling	10	1.5	15
Raspberry pi 3b+	1	80	80
Webcam	2	10	20
usb extension	2	3.5	7
PLA	2	24	48
Acid to burn the PCB	1	1	1
Copper Clad Laminate PCB	1	2	2
PCB Electronic components	1	10	10
DRV8825	3	5	15
Cable reel	1	20	16
Stainless steel 8mm shaft 1m	1	6	6
TOTAL			**$ 395.1**

Taking into account that the budget established by the company XTREGA3D to complete the project was $400, and the total cost of manufacturing the prototype was $395.1, it can be concluded that it was completed satisfactorily without exceeding the proposed budget.

REFERENCES

[1] A. Ali, “3d printer farm - robot-based automation,” 2021. [En línea]. Disponible: https://www.youtube.com/watch?v=EK57AHT1Xqkt=3s

[2] S. Aksnes, “Robotic solution to automate the 3D printing process,” May 2018. [En línea]. Disponible: https://www.youtube.com/watch?v=JmpPQA$_{8}aZc$

[3] A. Make, “Automatic 3d print removal using g-code,” 2019. [En línea]. Disponible: https://www.youtube.com/watch?v=avlengYsJdwt=1012s

[4] J. Huang, “Development of stepping motor driver based on drv8825,” in *2017 7th International Conference on Education, Management, Computer and Society (EMCS 2017)*. Atlantis Press, 2017, pp. 1866–1869.

[5] Myfuntech, “Creality pei sheet vs carborundum glass vs soft magnetic self-adhesive platform,” Jul 2021. [En línea]. Disponible: https://www.mytechfun.com/video/118

[6] J. L. Meriam, L. G. Kraige, y J. N. Bolton, *Engineering mechanics Dynamics*. John Wiley amp; Sons, 2020, p. 158.

[7] “Nema 23 stepper motor kh56km2u121 characteristics,” Mar 2019. [En línea]. Disponible: https://components101.com/motors/nema-23-stepper-motor-datasheet-specs

[8] “Nema 17 stepper motor 17hs3401 characteristics,” Mar 2017. [En línea]. Disponible: https://laborjag.com/venta/3d-printer-cnc/nema-17-stepper-motor-17hs3401/

[9] R. A. Ramos, “An algorithm for an iot prawn feeder in conjunction with an aquaponics system,” Ph.D. dissertation, 2020.

[10] N. Uke y R. Thool, “Moving vehicle detection for measuring traffic count using opencv,” *Journal of Automation and Control Engineering*, vol. 1, no. 4, 2013.